

1 Title Page

2 **Uncovering the Genetic Profiles Underlying the Intrinsic Organization of the**  
3 **Human Cerebellum**

4 **Running Title: Genetic substrates of cerebellar functional organization**

5 Yaping Wang<sup>1,2,3,4#</sup>, Lin Chai<sup>2,3,4#</sup>, Deying Li<sup>2,3,4</sup>, Chaohong Gao<sup>1,2,3,4</sup>, Congying Chu<sup>6</sup>,  
6 Zhengyi Yang<sup>2,3,4</sup>, Yu Zhang<sup>7</sup>, Junhai Xu<sup>8</sup>, Jens Randel Nyengaard<sup>1,9,10</sup>, Bing Liu<sup>6</sup>,  
7 Kristoffer Hougaard Madsen<sup>1,11,12</sup>, Tianzi Jiang<sup>1,2,3,4,5,13</sup>, Lingzhong Fan<sup>1,2,3,4,5\*</sup>

8 <sup>1</sup> Sino-Danish Center, <sup>2</sup> University of Chinese Academy of Sciences, Beijing 100190,  
9 China

10 <sup>3</sup> Brainnetome Center, <sup>4</sup> National Laboratory of Pattern Recognition, Institute of  
11 Automation, Chinese Academy of Sciences, Beijing 100190, China

12 <sup>5</sup> CAS Center for Excellence in Brain Science and Intelligence Technology, Institute  
13 of Automation, Chinese Academy of Sciences, Beijing 100190, China

14 <sup>6</sup> State Key Laboratory of Cognitive Neuroscience and Learning, Beijing Normal  
15 University, Beijing 100875, China

16 <sup>7</sup> Research Center for Healthcare Data Science, Zhejiang Lab, Hangzhou 311100,  
17 China

18 <sup>8</sup> School of Computer Science and Technology, Tianjin Key Laboratory of Cognitive  
19 Computing and Application, Tianjin University, Tianjin 300350, China

20 <sup>9</sup> Core Centre for Molecular Morphology, Section for Stereology and Microscopy,  
21 Department of Clinical Medicine, Aarhus University, Aarhus 8000, Denmark

22 <sup>10</sup> Department of Pathology, Aarhus University Hospital, Aarhus 8000, Denmark

23 <sup>11</sup> Informatics and Mathematical Modelling, Technical University of Denmark,  
24 Kongens Lyngby 2800, Denmark

25 <sup>12</sup> Danish Research Centre for Magnetic Resonance, Centre for Functional and  
26 Diagnostic Imaging and Research, Copenhagen University Hospital Amager and  
27 Hvidovre, Hvidovre 2650, Denmark

28 <sup>13</sup> School of Life Science and Technology, University of Electronic Science and  
29 Technology of China, Chengdu 610054, China

30 # Yaping Wang and Lin Chai contributed equally to this work.

31 **\*Corresponding Author:** Lingzhong Fan, Institute of Automation, Chinese Academy  
32 of Sciences, Beijing 100190, China. Email: [lingzhong.fan@ia.ac.cn](mailto:lingzhong.fan@ia.ac.cn), Phone: 010 -  
33 82544523.

## 34 **Abstract**

35 Decoding the genetic profiles underlying the cerebellar functional organization is  
36 critical for uncovering the essential role of the human cerebellum in various  
37 high-order functions and malfunctions in neuropsychiatric disorders. However, no  
38 effort has been made to systemically address this. By combining transcriptome data  
39 with the intrinsic functional connectivity of the human cerebellum, we not only  
40 identified 443 network-specific genes but also discovered that their gene  
41 co-expression pattern correlated strongly with intra-cerebellar functional connectivity.  
42 Of these genes, 90 were also differentially expressed in the cerebral cortex and linked  
43 the cortico-cerebellar cognitive-limbic networks. To further discover the biological  
44 functions of these genes, we performed a “virtual gene knock-out” by observing the  
45 change in the coupling between gene co-expression and functional connectivity and  
46 divided the genes into two subsets, i.e., a positive gene contribution indicator (GCI<sup>+</sup>)  
47 and a negative gene set (GCI<sup>-</sup>). GCI<sup>+</sup> is mainly involved in cerebellar  
48 neurodevelopment, while GCI<sup>-</sup> is related to neurotransmission and is significantly  
49 enriched in various neurological and neuropsychiatric disorders that are closely linked  
50 the cerebellar functional abnormalities. Collectively, our results provide new insight  
51 into the genetic substrates behind the functional organization of the human cerebellum  
52 with relevance to the possible mechanism of cerebellar contributions to related  
53 neurological and psychiatric disorders.

## 54 **Introduction**

55 Converging evidence from animal and human studies is advancing our understanding  
56 of the human cerebellum, which has been shown to be engaged in motor, complex  
57 cognitive, and emotional behaviors<sup>1,2</sup>. While such functional diversity of the  
58 cerebellum was believed to derive from its extensive afferent and efferent connections  
59 to extra-cerebellar structures, rather than being limited to a uniform cerebellar cortical  
60 cytoarchitecture<sup>1,3-6</sup>. It is well known that the macroscale functional organization of  
61 the human nervous system is widely accepted as being ultimately regulated by the  
62 underlying microscale gene expression<sup>7-10</sup>. Therefore, unraveling the genetic profiles  
63 underlying the cerebellar functional organization could help us understand how the  
64 cerebellum organizes different functional subregions that have homogeneous  
65 cytoarchitecture into functional networks that support its engagement in various  
66 functions<sup>11</sup> as well as increasing our understanding of its relevance in diverse brain  
67 diseases<sup>12,13</sup>.

68 However, the genetic mechanism supporting the functional organization of the  
69 human cerebellum is largely unknown. Only a few studies have attempted to  
70 investigate the genetic expression pattern of the human cerebellum, but they provided  
71 inconsistent results in terms of genetic expression variability. For instance, Hawrylycz  
72 et al.<sup>14</sup> and Negi and Guda<sup>15</sup> both found that gene expression is highly homogeneous  
73 across the anatomical regions of the healthy adult cerebellum. In contrast, Aldinger et  
74 al.<sup>16</sup> and Wang and Zoghbi<sup>10</sup> found that cerebellar development and function are

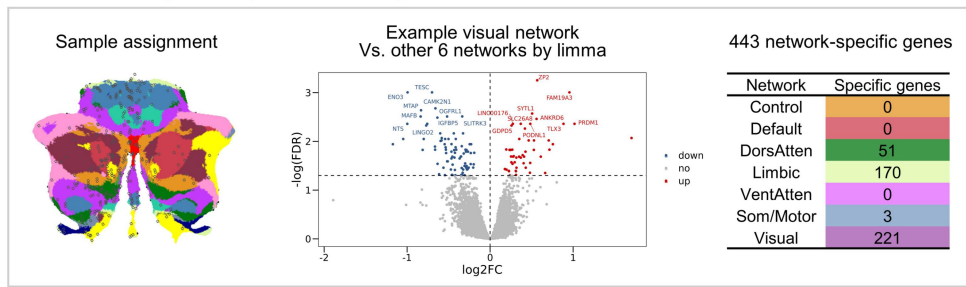
75 governed by the precise regulation of molecular and cellular programs and that the  
76 gene expression pattern is heterogeneous across spatial and temporal scales. In  
77 addition, differences in gene expression patterns between the cerebellar gyri and  
78 sulci<sup>17</sup>, and considerable cerebellar regional specializations containing specific cell  
79 types, as revealed by high-throughput single-nucleus RNA-seq<sup>18</sup> have been found in  
80 the mouse cerebellum. This inconsistency in the genetic variability of the cerebellum  
81 needs to be further explored because the relevant studies that showed homogeneity<sup>14,15</sup>  
82 only explored the overall cerebellar genetic expression pattern across its gross  
83 macro-anatomical boundaries (e.g., cerebellar lobules) and might have failed to fully  
84 reflect the functional organization of the human cerebellum<sup>19,20</sup>.

85 In the past decade, functional topological maps describing the organization of the  
86 human cerebellum using task<sup>21</sup> and task-free functional magnetic resonance imaging  
87 (fMRI)<sup>22,23</sup>, specifically, separate cerebellar functional networks<sup>22,23</sup> and  
88 intra-cerebellar functional gradients<sup>24</sup>, have been proposed. In particular, Buckner et  
89 al.<sup>22</sup> employed resting-state functional connectivity (rsFC) of the cerebello-cortical  
90 circuit as a tool to map the intrinsic functional architecture of the human cerebellum  
91 and proposed a possible functional parcellation into 7 networks and 17 networks. It is  
92 thus possible to decode the genetic profiles of cerebellar functional organization by  
93 investigating the molecular genetic substrates simultaneously linking cerebellar  
94 functional heterogeneity and its drivers, i.e., the connections. Whether and how the  
95 hypothesized determination of connections in cerebellar functional heterogeneity<sup>6</sup>  
96 interact with microscale gene expression is still an open question. To address this, one

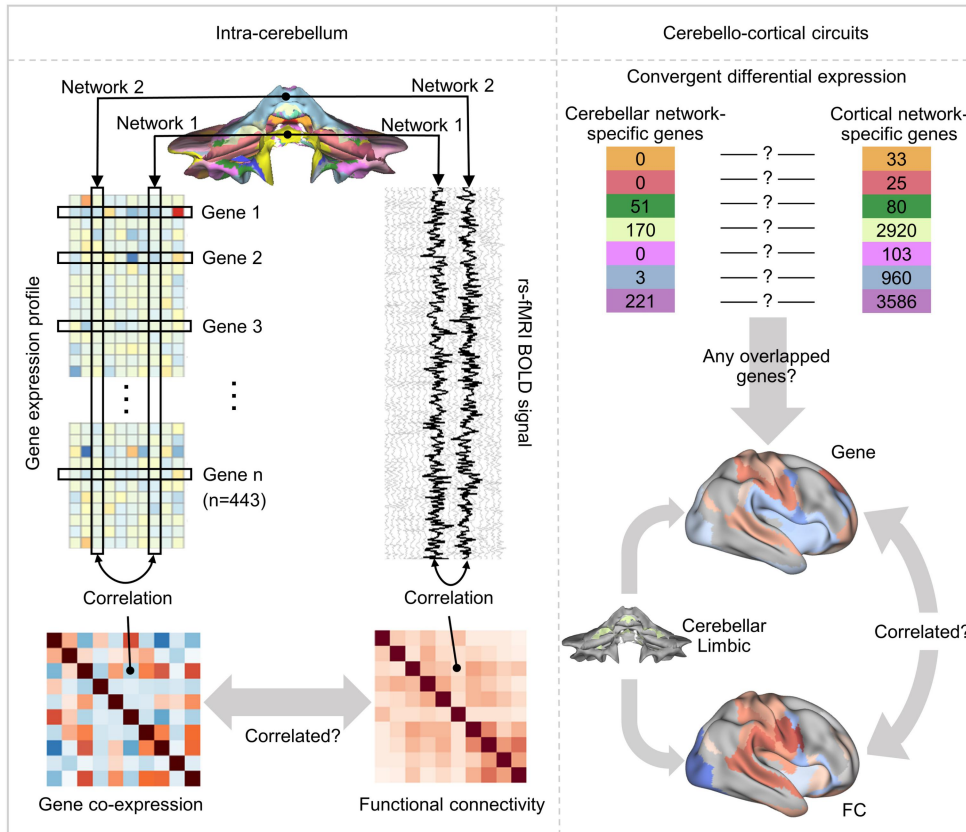
97 promising approach is imaging-transcriptomics analysis<sup>25-27</sup>, which allows the  
98 brain-wide spatial analysis of microscopic transcriptome data to be combined with  
99 macroscopic neuroimaging phenotypes<sup>7</sup>.

100 Thus, our goal was to investigate for the first time the neurobiological genetic  
101 mechanism underlying the functional organization of the human cerebellum to  
102 examine the correlation between the genes linking cerebellar functional heterogeneity  
103 and the functional integration of the human cerebellum. The schematic of the  
104 experimental design was shown in Fig. 1. Specifically, the Allen Human Brain Atlas  
105 (AHBA) transcriptome data<sup>7</sup> was combined with a cerebellar functional parcellation  
106 atlas<sup>22</sup> to identify the cerebellar network-specific genes (Fig. 1a). Then we found that  
107 the gene co-expression pattern of the network-specific genes showed a high  
108 correlation with the intra-cerebellar FC (Fig. 1b, left). In addition, we observed  
109 coupling between the gene co-expression of ~20% network-specific genes and FC  
110 across the cerebello-cortical limbic and control networks (Fig. 1b, right). Furthermore,  
111 by applying a series of functional annotation tools to these genes (Fig. 1c), we  
112 identified two gene sets separately involved in cerebellar neurodevelopment and  
113 neurotransmission and obtained interesting genetic evidence supporting the  
114 implications of cerebellar functional organization in many neurological and  
115 psychiatric disorders. The current exploration can provide a starting point in the effort  
116 to understand the molecular basis of cerebellar functional organization and open the  
117 door for investigating the pivotal role played by the cerebellum in many neurological  
118 and neuropsychiatric disorders.

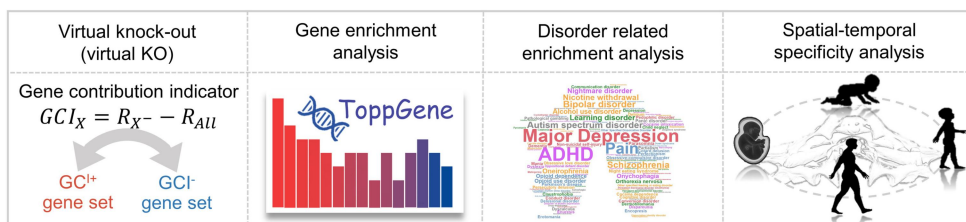
**a. Differential gene expression analysis**



**b. Correlation between FC and gene co-expression**



**c. Functional annotation**



119

120 **Fig. 1 | Analysis pipeline.** a Differential gene expression analysis. We assigned the  
 121 AHBA cerebellar samples into 7 cerebellar functional networks (left)<sup>22</sup> and averaged  
 122 each gene's expression within the same network individually. Then we compared the  
 123 gene expression in each network with all the other networks by limma<sup>28</sup> (middle) with

124 a fold change  $> 0$  and FDR corrected  $p < .05$  as an indicator (Red indicates that the  
125 genes we found were significantly positively expressed in the visual network.). Thus,  
126 we obtained the network-specific genes for 7 networks (right). **b** Correlations between  
127 the gene co-expression and the FC included intra-cerebellar and cerebello-cortical  
128 circuits. Intra-cerebellum: for each pair of networks, we calculated the gene  
129 expression similarity between them using 443 cerebellar network-specific genes and  
130 then constructed the gene co-expression matrix. The FC matrix was constructed by  
131 correlating the BOLD signal for all pairs. Then the relationship between the genetic  
132 correlation and functional correlation was evaluated. Cerebello-cortical circuits: We  
133 first defined the cortical network-specific genes as we had for the cerebellum and  
134 tested whether any convergently expressed genes occurred. Then we used the  
135 overlapping genes to obtain the cortical genetic correlation for each cerebellar  
136 network and evaluated the relationship between the cortical genetic and functional  
137 correlation for each cerebellar network. **c** Functional annotation includes virtual  
138 knock-out (KO), gene enrichment analysis, disorder-related enrichment analysis, and  
139 spatial-temporal specificity analysis.

## 140 **Results**

### 141 *The cerebellar network-specific genes derived based on the functional segregation* 142 *within the cerebellum*

143 The genes that were expressed much more in one network than in all the other six  
144 networks in the cerebellum and cerebral cortex were identified based on the  
145 differential gene expression analysis and are referred to as cerebellar network-specific  
146 genes and cortical network-specific genes, respectively. We identified 443 cerebellar  
147 network-specific genes (Supplementary sheet 2, 3) using all samples from 6 donors



148 across 7 networks. The distribution of these network-specific genes is shown in Table  
149 1, which shows that these were mainly expressed in the limbic ( $n = 170$ ), dorsal  
150 attention ( $n = 51$ ), somato/motor ( $n = 3$ ), and visual ( $n = 221$ ) networks. We also  
151 obtained 6,987 cortical network-specific genes (Supplementary sheet 5, 6, Table 1)  
152 using the same strategy and found that the cerebellar and cortical network-specific  
153 genes distribution patterns were highly correlated ( $r = 0.95$ ,  $p = .00108$ ).

154 Moreover, we found that 90 of these 443 cerebellar network-specific genes (~  
155 20%) (Supplementary sheet 7, 8, Table 1) were convergently expressed in the cerebral  
156 cortex and that a significant overlap between the cerebellar and cortical  
157 network-specific genes of the limbic and somatomotor networks occurred (limbic  
158 overlap = 56, hypergeometric  $ps < .0001$ ; somatomotor overlap = 2, hypergeometric  
159  $ps < .01$ ). This means that the 56 limbic genes were differentially expressed in the  
160 limbic cortex and the limbic cerebellum and that the 2 somatomotor genes were  
161 differentially expressed in the somatomotor cortex and somatomotor cerebellum.  
162 Overlapped genes were also found in the visual network but failed to pass the  
163 hypergeometric test (visual overlap = 33, with hypergeometric  $ps = .84$ ), and no  
164 overlap was found for the other 4 networks (ventral attention, dorsal attention, control,  
165 default, Supplementary sheet 7).

		Cerebellum	Cortex	Overlap genes
Control		0	33	0
Default		0	25	0
Dorsal Attention		51	80	0
Limbic		170	2920	56*
Ventral Attention		0	103	0
SomatoMotor		3	960	2*
Visual		221	3586	33
Total (unique)		443	6987	90

166

167 **Table 1 | Counts of significantly expressed genes within each network compared**  
168 **to other networks** (referred to as network-specific genes for simplicity). Here we  
169 defined the cerebellar ( $n = 443$ , left column, Supplementary sheets 2, 3) and cortical  
170 network-specific genes ( $n = 6987$ , middle column, Supplementary sheets 5, 6) across  
171 the cerebellar<sup>22</sup> and cortical<sup>29</sup> 7-network strategies. The rightmost column measures  
172 the overlap between the cerebellar and cortical network-specific genes for each  
173 network (Supplementary sheets 7, 8), \* Hypergeometric  $ps \leq .01$ .

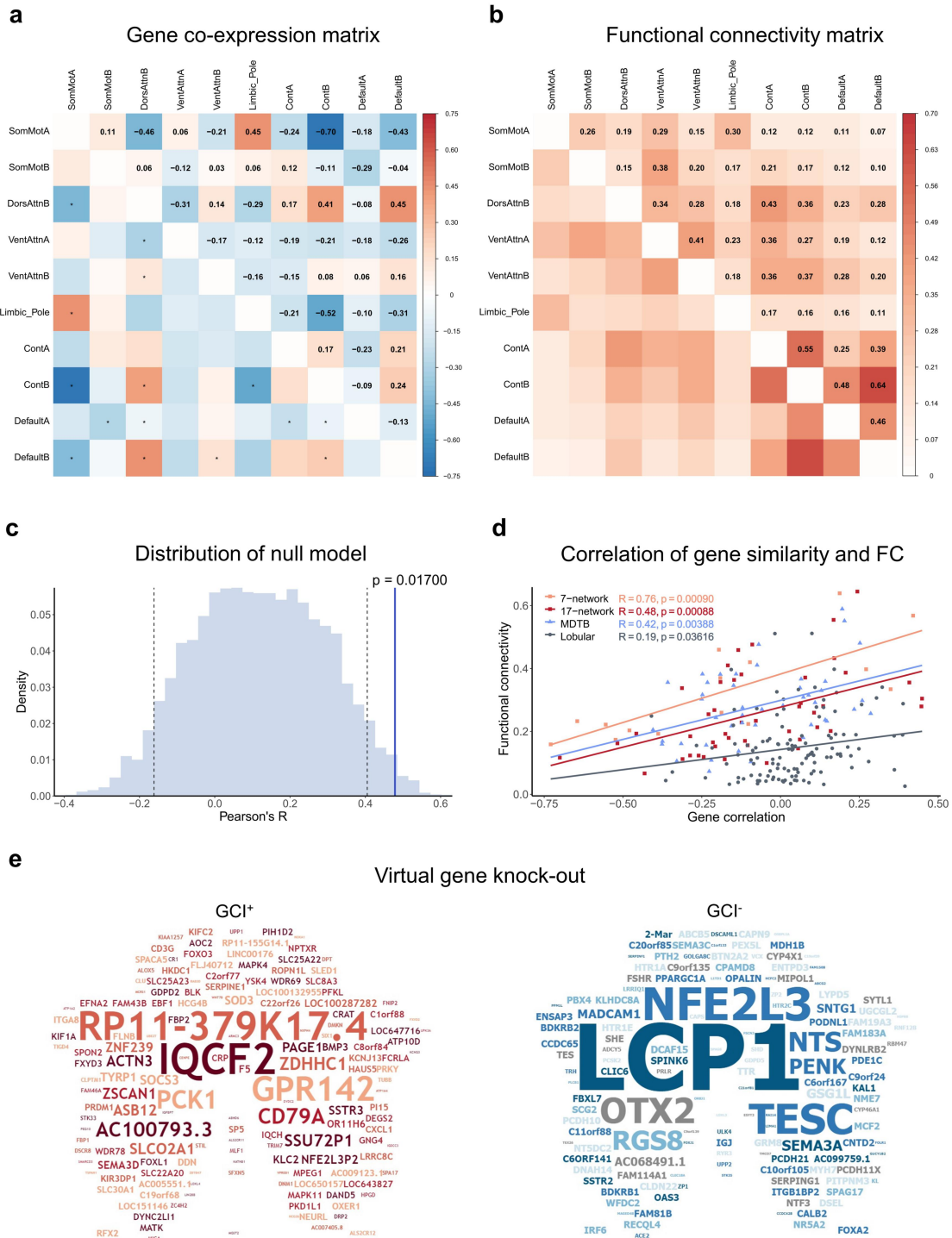
174 *The co-expression of the cerebellar network-specific genes highly correlated with*  
175 *intra-cerebellar FC*

176 Using the 443 cerebellar network-specific genes, we constructed the gene  
177 co-expression matrix for the 2 bi-hemisphere donors and explored the relationship  
178 between gene correlation and FC within the cerebellum. Across all the available  
179 network-network pairs, the genetic co-expression correlates with the FC within the  
180 cerebellum ( $r = 0.48$ ,  $p = .00088$ , with permutation test  $p = .01700$ , Fig. 2). The  
181 genetic correlations were either positive or negative, but the FCs were all positive,  
182 and the negative genetic correlation corresponded to a mild functional correlation (Fig.  
183 2d, red). This correlation between gene co-expression and FC was referred to as

184 Gene-FC correlation throughout present paper for simplicity. To validate the Gene-FC  
185 correlation within the cerebellum, we also leveraged the task-free 7-network  
186 parcellation, task-based multi-domain task battery (MDTB) functional parcellation<sup>21</sup>,  
187 and the cerebellar lobular parcellation<sup>30</sup> to re-perform the aforementioned steps (Fig.  
188 2d). The gene co-expression and FC within the cerebellum also correlated when  
189 analyzed based on the 7-network parcellation ( $r = 0.76$ ,  $p = .00090$ , Fig. 2d,  
190 Supplementary Fig. 1), the MDTB functional parcellation ( $r = 0.42$ ,  $p = .00388$ , Fig.  
191 2d, Supplementary Fig. 2), and the cerebellar lobular parcellation ( $r = 0.19$ ,  $p$   
192  $= .03616$ , Fig. 2d, Supplementary Fig. 3). The Gene-FC correlation for the lobular  
193 parcellation, however, failed to pass the Bonferroni corrected significance level ( $p$   
194  $< .05$ ). This is consistent with the observation that, compared with cerebellar  
195 morphological boundaries, a functional atlas performs better in terms of functional  
196 representativeness<sup>19,20</sup>.

197 Therefore, the 443 cerebellar network-specific genes that we derived based on the  
198 functional segregation of the cerebellum also correlated with the functional  
199 integration of the cerebellum. This Gene-FC correlation was not generated by chance,  
200 so it was consistent using a different parcellation resolution and independent  
201 cerebellar functional atlas although it disappeared in the lobular parcellation.  
202 Moreover, the control test exhibited no Gene-FC correlation when the gene  
203 co-expression was constructed using non-network-specific genes (Supplementary  
204 sheet 28) regardless of whether the test was thresholdless or thresholded. These  
205 findings further confirmed that these 443 network-specific genes play a key role in

206 intra-cerebellar functional organization.



207

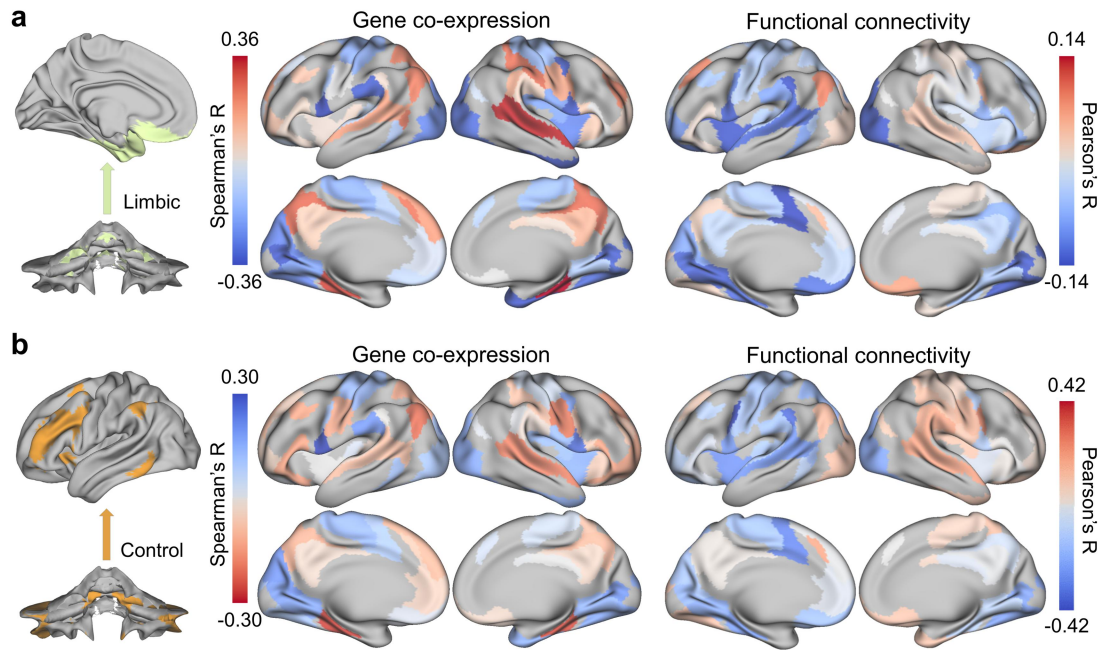
208 **Fig. 2 | Network-specific gene co-expression correlates with functional**  
 209 **connectivity (FC) within the cerebellum. a** Genetic correlation was shown by the  
 210 co-expression matrix (Supplementary sheet 9) constructed for two bi-hemisphere  
 211 donors across 10 cerebellar networks using 443 cerebellar network-specific genes

212 derived from all six donors. The 10 cerebellar networks corresponded to the networks  
213 containing samples from both bi-hemisphere donors (Supplementary Table 3).  
214 Genetic correlation revealed both positive (red) and negative (blue) correlations, \*  
215 Bonferroni corrected  $p \leq .05$ . **b** The FC matrix (Supplementary sheet 10) shows the  
216 functional correlation for the 10 cerebellar networks using 1,018 subjects from the  
217 HCP S1200 release<sup>31</sup>. They were positively correlated with each other, and all passed  
218 the Bonferroni corrected significant threshold  $p \leq .0001$ . **c** Distribution of the null  
219 model constructed using a permutation test that evaluated whether our Gene-FC  
220 correlation was generated by chance. The vertical black dashed lines correspond to the  
221  $p$  values of .05 and .95; our observed Gene-FC correlation, shown by the blue vertical  
222 line, corresponds to  $p = .01700$ . **d** The overall intra-cerebellar Gene-FC correlation  
223 using different parcellations: task-free 7-network (orange) and 17-network (red)  
224 parcellation of the cerebellar functional atlas based on the cerebello-cortical rsFC,  
225 task-based MDTB functional parcellation (blue) based on the task activation pattern,  
226 and cerebellar lobular parcellation (grey). The Pearson's correlation  $R$  and  $p$  values  
227 are shown by corresponding colors. **e** The  $GCI^+$  ( $n = 246$ , left) and  $GCI^-$  ( $n = 197$ ,  
228 right) gene list were displayed on flattened shape of the cerebellum.

229 ***Convergently expressed genes among the cerebellar and cortical network-specific***  
230 ***genes correlated with the FC across the cerebello-cortical cognitive-limbic networks***

231 Since 90 of the 443 cerebellar network-specific genes were convergently expressed  
232 across the cerebello-cortical circuit, we wanted to know whether these ~20% genes  
233 correlated with the FC across the cerebello-cortical circuit. A correspondence between  
234 the genetic and functional correlations was identified for the limbic ( $r = 0.36$ , FDR  
235 corrected  $p = .03026$ , Fig. 3a) and control networks ( $r = -0.33$ , FDR corrected  $p$   
236 = .03449, Fig. 3b) but was not significant for the somatomotor ( $r = -0.15$ , FDR

237 corrected  $p = .39433$ ), dorsal attention ( $r = -0.19$ , FDR corrected  $p = .28134$ ), ventral  
238 attention ( $r = -0.04$ , FDR corrected  $p = .77856$ ), or default ( $r = 0.10$ , FDR corrected  $p$   
239 =  $.54382$ ) networks. The high cortical genetic similarity between the limbic system  
240 and the adjacent control network ( $r = -0.90$ , FDR corrected  $p < .0001$ ), somatomotor  
241 network ( $r = -0.55$ , FDR corrected  $p < .0001$ ), and ventral attention network ( $r = -0.72$ ,  
242 FDR corrected  $p < .0001$ ) indicates that the gene co-expression between the cerebellar  
243 limbic network and the cortex reflects a gradual genetic gradient rather than genetic  
244 dissimilarity between the cerebellar limbic network and the other cerebellar networks.  
245 In addition, while controlling the effect of the cortical genetic similarity between the  
246 limbic and control networks, the partial correlation showed no cortical Gene-FC  
247 correlation for the control network ( $r = -0.13$ ,  $p = .31596$ ), which implies that the  
248 significant cortical Gene-FC correlation for the control network was induced by the  
249 high cortical genetic similarity between the cerebellar limbic and control networks.  
250 This is also consistent with the finding that convergently expressed genes were only  
251 observed in the limbic network, but not in the control network (Table 1). Overall,  
252 these 443 cerebellar network-specific genes not only correlated with the  
253 intra-cerebellar FC, but ~20% of them were also linked with the cerebello-cortical  
254 cognitive-limbic networks.



255

256 **Fig. 3 | Genetic and functional cortical correlation of limbic and control**

257 **cerebellar networks seeds.** Both were calculated for 2 bi-hemisphere donors across

258 10 cerebellar networks and 59 cortical parcels that contained samples from both

259 bi-hemisphere donors. **a** Limbic: The cortical gene co-expression (Supplementary

260 sheet 11) was calculated using the 90 overlapping genes between the cerebellar and

261 cortical network-specific genes by Spearman's correlation. The FC across each

262 cerebellar network with each cortical parcel was calculated using Pearson's

263 correlation (Supplementary sheet 12). The cortical limbic genetic and functional

264 correlations were correlated with each other ( $r = 0.36$ , FDR corrected  $p = .03026$ ). **b**

265 Control: The cortical gene co-expression and the FC for the control network were

266 correlated with each other ( $r = -0.33$ , FDR corrected  $p = .03449$ ). Noted, the color bar

267 of gene co-expression was inverted considering the negative Gene-FC correlation for

268 the control network.

269 ***Functional annotation revealed distinct biological properties of GCI<sup>+</sup> and GCI<sup>-</sup>***  
270 ***separated by virtual KO***

271 In addition to the overall correlation between gene co-expression and the functional  
272 integration of the cerebellum, we investigated each gene's importance to the  
273 intra-cerebellar Gene-FC correlation by scoring the 443 cerebellar network-specific  
274 genes based on the gene contribution indicator (GCI). Using the virtual gene  
275 knock-out (KO) procedure, we were able to classify the 443 network-specific genes  
276 that linked cerebellar functional segregation and integration into two groups: a 246  
277 GCI positive gene set (GCI<sup>+</sup>, Fig. 2e left, Supplementary sheet 13) and a 197 GCI  
278 negative gene set (GCI<sup>-</sup>, Fig. 2e right, Supplementary sheet 14). The distinction  
279 between the two sets is that the virtual KO of GCI<sup>+</sup> genes increased the Gene-FC  
280 correlation, whereas the virtual KO of GCI<sup>-</sup> genes decreased the Gene-FC correlation.  
281 Based on the winner-take-all principle, GCI<sup>-</sup> genes may have a critical impact on the  
282 functional organization of the cerebellum; an example is that the top genes, LCP1 and  
283 TESC, enable GTPase binding and calcium binding, respectively<sup>32</sup>, which are key  
284 functions within signaling transduction. Therefore, we applied a range of  
285 bioinformatics tools to further explore the underlying roles of the GCI<sup>+</sup> and GCI<sup>-</sup>.

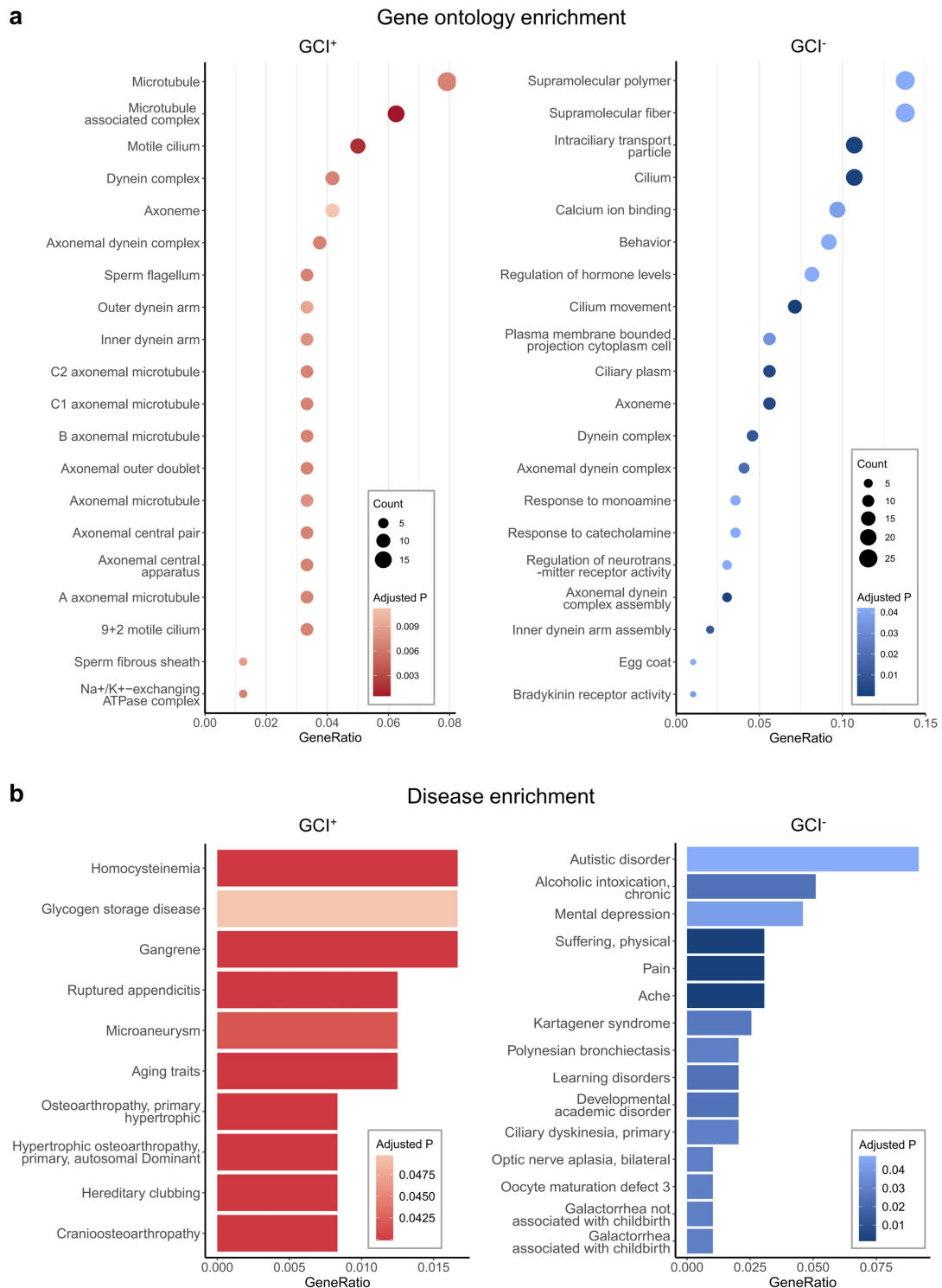
286 The gene ontology (GO) enrichment analysis of the GCI<sup>+</sup> and GCI<sup>-</sup> is shown in  
287 Fig. 4a. The GCI<sup>+</sup> was mainly enriched in microtubule-related terms, including the  
288 microtubule associated complex (ID: 0005875, FDR corrected  $p = .00050$ ), motile  
289 cilium (ID: 0031514, FDR corrected  $p = .00156$ ), and dynein complex (ID:



290 GO:0030286, FDR corrected  $p = .00678$ ). Compared with GCI<sup>+</sup>, the GCI<sup>-</sup> was not  
291 only enriched in microtubule-related terms but was also significantly enriched in  
292 terms related to neurotransmitter transport, such as calcium ion binding (ID: 0005509,  
293 FDR corrected  $p = .03709$ ), regulation of hormone levels (ID: 0010817, FDR  
294 corrected  $p = .04195$ ), response to catecholamine (ID: 0071869, FDR corrected  $p$   
295 =  $.04195$ ), response to monoamine (ID: 0071867, FDR corrected  $p = .04195$ ), and  
296 regulation of neurotransmitter receptor activity (ID: 0099601, FDR corrected  $p$   
297 =  $.04195$ ). This is consistent with their different pathway enrichment results  
298 (Supplementary sheets 15,16) in that the GCI<sup>+</sup> was primarily enriched in some basic  
299 biological pathways: proximal tubule bicarbonate reclamation (ID: M4361, FDR  
300 corrected  $p = .03197$ ) and glycolysis/gluconeogenesis (ID: M39474, FDR corrected  $p$   
301 =  $.03197$ ), which provides the energy need during microtubule-related processes. In  
302 contrast, the GCI<sup>-</sup> was primarily involved in signaling transduction, especially in  
303 some neurotransmission pathways, such as the neuroactive ligand-receptor interaction  
304 (ID: M13380, FDR corrected  $p = .03877$ ).

305 Since the GCI<sup>+</sup> and GCI<sup>-</sup> are involved in different biological processes, we  
306 hypothesized that they also play different roles in brain disease or related to different  
307 brain diseases. Unexpectedly, we found no link between GCI<sup>+</sup> and any brain-related  
308 illnesses (Fig. 4b, left) but observed an involvement of GCI<sup>-</sup> in various neurological  
309 and neuropsychiatric disorders (Fig. 4b, right), including autistic disorder (ID:  
310 C0004325, FDR corrected  $p = .04734$ ), alcoholic intoxication (ID: C0001973, FDR  
311 corrected  $p = .02349$ ), mental depression (ID: C0011570, FDR corrected  $p = .04167$ ),

312 pain (ID: C0030193, FDR corrected  $p = .00141$ ), learning disorders (ID: C0023186,  
313 FDR corrected  $p = .02349$ ) and others. Many of these, especially mental depression  
314 and autistic disorder, have a close relationship with the human cerebellum, in which  
315 patients have shown functional connectivity abnormalities<sup>33,34</sup>. The mental  
316 depression- and autistic disorder-associated genes were TRH, PENK, TTR, ADCY5,  
317 NRXN1, HTR1A, HTR2C, NTS, PEX5L ( $n = 9$ , Supplementary sheet 16) and  
318 DLGAP2, TRH, PENK, RYR3, SEMA3A, NRXN1, TESC, ABCG2, PCDH10,  
319 CNTN4, HTR1A, CALB2, HTR2C, DNAAF4, FOLR1, NTS, GRM8, UPP2 ( $n = 18$ ,  
320 Supplementary sheet 16), respectively, and the overlapping genes were TRH, PENK,  
321 NRXN1, HTR1A, HTR2C, NTS ( $n = 6$ ).

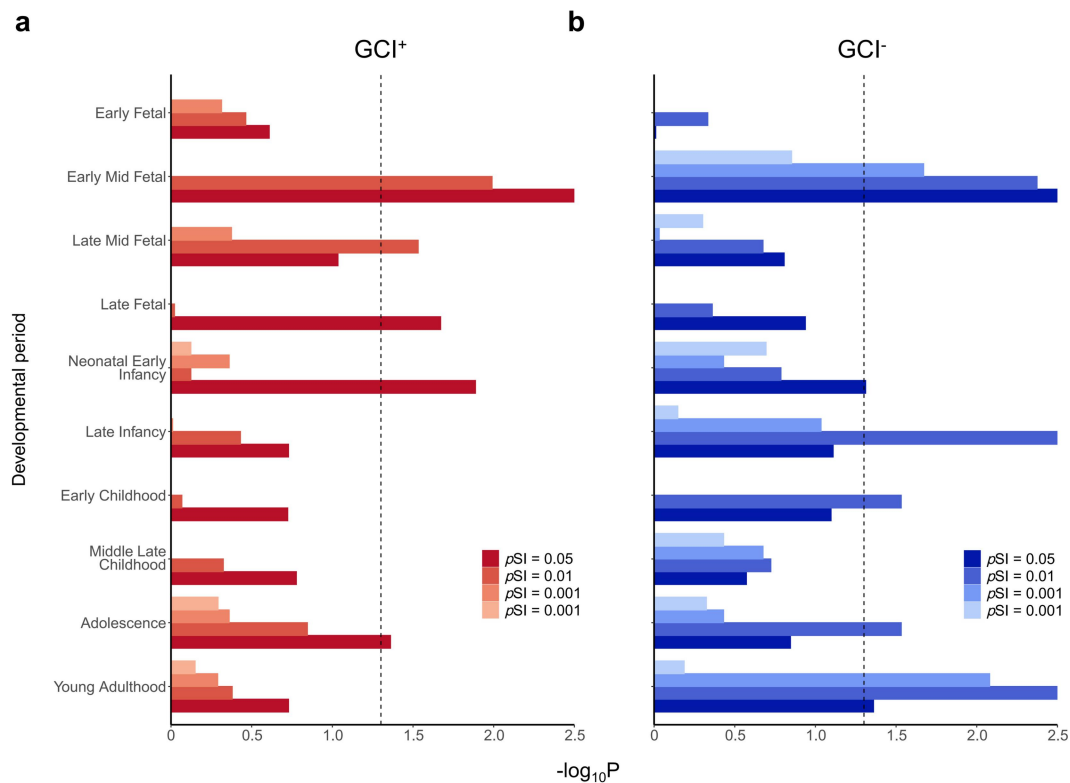


322

323 **Fig. 4 | The gene ontology (GO) and disease enrichment analysis for GCI<sup>+</sup> and**  
 324 **GCI<sup>-</sup>.** a Bubble plot shows the GO enrichment top 10 terms for GCI<sup>+</sup> (left) and GCI<sup>-</sup>  
 325 (right) (all results are shown in Supplementary sheets 15 and 16, respectively). The  
 326 biological process (BP), cellular component (CC), and molecular function (MF) are

327 displayed together. The dot size (count) represents the number of genes that are within  
328 the interest GCI<sup>+</sup> or GCI<sup>-</sup> gene panels as well as a specific GO term (y-axis). The  
329 color shows the FDR corrected *p* value. **b** Gradient barplot showing the disease  
330 enrichment for all representative results for GCI<sup>+</sup> and top 15 representative terms for  
331 GCI<sup>-</sup>. The color represents the FDR corrected *p* value.

332 In light of the distinct properties of GCI<sup>+</sup> and GCI<sup>-</sup>, we wanted to know whether  
333 the roles played by these two gene sets showed variable prevalence at different ages.  
334 By leveraging the BrainSpan dataset<sup>35</sup> and applying the analysis strategy of CSEA  
335 tool<sup>36</sup>, we found that GCI<sup>+</sup> showed significant overexpression in early middle fetal,  
336 late middle fetal, late fetal, and neonatal early infancy compared with GCI<sup>-</sup> (Fig. 5a).  
337 These stages neatly correspond to the timeline of the protracted development of the  
338 human cerebellum<sup>37</sup>, which extends from the early embryonic period until the end of  
339 the first postnatal year. This appears to be consistent with the observation that the  
340 GCI<sup>+</sup> is involved in some fundamental biological processes, especially  
341 microtubule-related activity, whose dynamics play a key role in cerebellar  
342 neurodevelopment<sup>38</sup>. In contrast, compared with the GCI<sup>+</sup>, the GCI<sup>-</sup> was significantly  
343 expressed in late infancy, early childhood, adolescence, and young adulthood (Fig.  
344 5b), which includes the highest neurodevelopmental risk windows for autism  
345 spectrum disorder (ASD)<sup>39</sup> and major depression disorder (MDD)<sup>40</sup>, both of which we  
346 found in the disease enrichment analysis.



347

348 **Fig. 5 | Integrative spatial-temporal specificity analysis of GCI<sup>+</sup> (a) and GCI<sup>-</sup> (b)**  
349 **within the cerebellum.** The specificity index probability ( $pSI = .05, .01, .001,$   
350  $\text{and } .0001$ , permutation corrected, shown as different colors) was used to determine  
351 how likely a gene was to be expressed in a given time window relative to all other  
352 time windows<sup>36</sup>. The x-axis corresponds to the  $-\log_{10}$  (FDR corrected  $p$  value), and  
353 for aesthetics if  $-\log_{10}$  (FDR corrected  $p$  value)  $> 2.5$ ,  $-\log_{10}$  (FDR corrected  $p$  value)  
354  $= 2.5$ ; the y axis represents the 10 development windows collected by BrainSpan<sup>35</sup>.  
355 The vertical dark dashed line corresponds to the FDR corrected  $p = .05$ . All results are  
356 shown in Supplementary sheet 17.

## 357 Discussion

358 The current study provided a first tentative exploration of the genetic differential and  
359 co-expression linked with the functional organization of the human cerebellum

360 and has the potential for elaborating and rethinking the neurobiological underpinnings  
361 of the cerebellar functional organization. Furthermore, we identified two gene sets  
362 involved in cerebellar neurodevelopment and neurotransmission and found interesting,  
363 indirect genetic evidence supporting the key role played by the cerebellar functional  
364 network in many neurological and psychiatric disorders, which hints at a possible  
365 mechanistic explanation for the cerebellar contributions to related neurological and  
366 psychiatric disorders.

367 ***The genetic profiles underlying cerebellar functional segregation correlate with***  
368 ***intra-cerebellar and cerebello-cerebral connections***

369 In this study we found correlations between the identified cerebellar network-specific  
370 genes and the intra-cerebellar connection and cerebello-cerebral FC. These findings  
371 could provide possible empirical genetic support for the hypothesized decisive role of  
372 cerebellar connectivity in the functional heterogeneity of the cerebellum. First, while  
373 obtaining the network-specific genes, we found significant differences in the number  
374 of identified genes between the functional specificity (i.e., limbic, visual networks)  
375 and functional diversity networks (i.e., the control, default networks); specifically,  
376 more differentially expressed genes were in the former and vice versa in the latter<sup>41</sup>.  
377 This was also found in a previous cortical gene expression homogeneity analysis<sup>7</sup> that  
378 showed that a relatively high differential expression pattern was observed in the  
379 primary sensory cortex, area 38, and the primary visual cortex, a finding that closely  
380 corresponds with the somatomotor, limbic, and visual networks. But the findings

381 related to the inconsistency in the amount of somatomotor cerebellar ( $n = 3$ ) and  
382 somatomotor cortical network-specific genes ( $n = 960$ ) were not completely clear.  
383 One possible explanation may be that the preferential links between the cerebellar  
384 representations of body space and the motor, somatosensory, and premotor cortices  
385 are difficult to distinguish<sup>22</sup>. The cerebellar network-specific genes we obtained are  
386 not in keeping with the highly homogeneous gene expression within the human  
387 cerebellum suggested by its anatomic atlas<sup>7,14</sup>. Even though we selected a definition of  
388 differentially expressed genes using an FDR corrected statistical threshold rather than  
389 an arbitrary threshold and although lobule-specific genes were identified using our  
390 statistical threshold, these genes did not correlate with the FC of the human  
391 cerebellum. This indicates that the arbitrary fold change threshold was not appropriate  
392 for determining biologically meaningful but subtle differences<sup>42</sup> and that the genes  
393 underlying the lobular segregation are not related to the resting-state activity of the  
394 human cerebellum. These findings support, from a genetic perspective, the idea that  
395 the morphological subdivisions of the cerebellum do not correspond well to its  
396 functional representation<sup>19,20</sup>.

397       Second, the overall distribution patterns of the cerebellar and cortical  
398 network-specific genes were highly correlated, a finding that is consistent with a  
399 similar macroscale principle that was identified in the cerebellar and cortical  
400 functional organization<sup>24,43</sup>. These correlated patterns may be related to the way that  
401 we defined the cerebellar network, which was by projecting the cerebral cortical  
402 networks onto the cerebellum by computing the functional connections between the

403 two regions<sup>22</sup>. More interestingly, the molecular genetic substrates simultaneously  
404 linking functional heterogeneity and integration could only be observed across the  
405 functional subdivision, regardless of whether the parcellation was based on the  
406 task-free cerebello-cortical rsFC<sup>22</sup> or the intra-cerebellar task-based activation  
407 pattern<sup>21</sup>, but disappeared in the lobular parcellation. These interpretations are further  
408 supported by the widely accepted notion about the human cerebellum that its  
409 functional specialization is dominated by its connection with extracerebellar  
410 structures rather than within its homogeneous cytoarchitecture<sup>6</sup>. Although no  
411 intra-cerebellar anatomical fiber connections linking adjacent or distant cerebellar  
412 regions with each other have been found<sup>44,45</sup>, it is widely accepted that the  
413 intra-cerebellar functional map is a consequence of the topological arrangement of its  
414 extra-cerebellar anatomical connections<sup>6</sup>. This proposed relationship between extra-  
415 and intra-cerebellar connectivity can in turn be expected to affect the resting-state  
416 activity between cerebellar regions<sup>24</sup>.

417 Third, in addition to the intra-cerebellar Gene-FC correlation, we observed a  
418 direct correlation between genes underlying the cerebellar functional specialization  
419 and cerebello-cerebral FC with respect to the limbic and control networks. The  
420 Gene-FC correlation in the control network was mainly caused by the genetic  
421 similarity between these two networks; this interaction between limbic-emotion and  
422 control-cognition has been confirmed both anatomically and behaviorally<sup>46</sup>. For  
423 instance, the integrated processing by the emotion and cognition areas has been  
424 identified solely based on their anatomical connections<sup>47</sup>. This relationship can also be



425 observed in that, when looking at the top of a hill, a sad mood induces a steeper  
426 perception of the hill than a happy one<sup>48</sup>. One possible reason why we only obtained  
427 this correspondence in the limbic network may be the low functional heterogeneity<sup>41</sup>  
428 and inter-individual functional variability<sup>49</sup> of the limbic network compared with  
429 others as well as the complexity of gene expression; i.e., the Gene-FC correlation is  
430 not fully portrayed by the differentially expressed genes<sup>27</sup>. Considering the large  
431 differences between the cerebellum and cortex in terms of their gene expression  
432 patterns<sup>14</sup> and structure-function relationships<sup>50</sup> as well as the individual variability of  
433 their functional networks<sup>51</sup>, identifying 90 convergently expressed genes that linked  
434 the cerebello-cortical cognitive-limbic networks is very significant and may hold  
435 clues to the molecular underpinnings of the cognitive-emotion roles played by the  
436 cerebello-cortical circuit. For example, the HTR1A and HTR2C, which are both  
437 preferentially expressed in the cerebellar and cortical limbic network, are pivotal  
438 genes in serotonin transmission, play a modulation role in the limbic system, and act  
439 as important therapeutic targets in limbic system-related disorders<sup>52</sup>.

440 *Cerebellar neurodevelopment features of GCI<sup>+</sup>, cerebellar neurotransmission,*  
441 *neurological, and neuropsychiatric disorders-related features of GCI<sup>-</sup>*

442 Interestingly, we derived two gene subsets with pronouncedly different characteristics  
443 based only on the direction in which each gene influenced the intra-cerebellar  
444 Gene-FC correlation by applying a simple virtual KO approach on the 443 cerebellar  
445 network-specific genes. By using a series of bioinformatic tools, we found converging

446 evidence for GCI<sup>+</sup> and GCI<sup>-</sup> involvement in cerebellar neurodevelopment and  
447 cerebellar neurotransmission, respectively. It is also interesting to speculate that these  
448 443 network-specific genes that link both cerebellar functional segregation and  
449 integration have a relationship with some brain-related disorders since prior evidence  
450 showed that the cerebellar functional organization plays a key role in various  
451 neurological<sup>13,53</sup> and neuropsychiatric disorders<sup>12</sup>, most of which possess common  
452 underlying genetic risks<sup>54</sup>. But a tricky problem emerged in that the genes we are  
453 interested in were derived from healthy individuals. This could be tackled to some  
454 extent by using the virtual KO method, which can simulate the different expression  
455 levels of each gene and thus coarsely corresponds to a fraction of the expression level  
456 under normal health and disease situations. This is why we thought that we might be  
457 able to see whether the GCI<sup>+</sup> and GCI<sup>-</sup> are related to a specific disease even though  
458 the genes were derived from healthy individuals.

459 The GCI<sup>+</sup> is involved in many microtubule-related terms and is overexpressed  
460 throughout the protracted development of the cerebellum. The dynamics and  
461 flexibility of microtubules were found to be essential throughout cerebellar  
462 development because they affect the morphological alterations of Purkinje cells<sup>38</sup>. In  
463 addition, some genes of the GCI<sup>+</sup>, such as GTPBP2<sup>55</sup> and Lin28b<sup>56</sup>, were found to  
464 play a key role in neurodevelopment; overexpression of the Lin28b gene can induce  
465 the development of pathological lobulation in the cerebellum<sup>56</sup>. This converging  
466 evidence prompts our speculation that the GCI<sup>+</sup> is engaged in cerebellar  
467 neurodevelopment. Unexpectedly, the GCI<sup>+</sup> showed no link to brain-related diseases,

468 which appears to be consistent with its primary involvement in many fundamental  
469 biological functions. However, this lack of disease linkage is inconsistent with the  
470 significant overexpression of GCI<sup>+</sup> genes during the protracted development of the  
471 cerebellum, in that many researchers pointed out that this protracted development  
472 increased the susceptibility of the cerebellum to many psychiatric disorders<sup>37</sup>. This  
473 likely is complemented by the overexpression of GCI<sup>-</sup> in the early middle fetal and  
474 neonatal early infancy periods. Other possible explanations include that there are few  
475 genetic studies of the cerebellum compared with the cerebral cortex as well as large  
476 genetic expression differences between the cerebellum and extra-cerebellar  
477 structures<sup>14</sup>, so the related datasets may lack sufficient information that is specific to  
478 the cerebellum. This calls for future studies seeking to provide a more complete  
479 explanation by considering multiple perspectives.

480 The GCI<sup>-</sup> was found to be involved in many neurotransmission processes,  
481 enriched in various neurological and psychiatric disorders, and significantly  
482 overexpressed in late infancy, early childhood, adolescence, and young adulthood  
483 compared with GCI<sup>+</sup>. These results are mutually supportive. Neurotransmission has  
484 long been thought to play a crucial role in various neurological<sup>57</sup> and neuropsychiatric  
485 disorders<sup>58,59</sup>. For example, the abnormal transmission of monoamines and  
486 catecholamines, such as serotonin and dopamine, has been widely linked with many  
487 psychiatric disorders, and these transmitters have thus become potential treatment  
488 targets<sup>60</sup>. The time period through which the GCI<sup>-</sup> genes are expressed includes the  
489 high-risk time windows for GCI<sup>-</sup>-enriched disorders, such as mental depression (aged

490 18–29)<sup>40</sup> and autistic disorder (from infancy to childhood)<sup>39</sup>, and the high expression  
491 of GCI in early middle fetal life might be associated with the prenatal risk factors  
492 associated with depression<sup>61</sup> and autism<sup>62</sup>.

493 Moreover, we found that the GCI was enriched in many neurological and  
494 neuropsychiatric disorders including mental depression, autistic disorder, pain,  
495 alcoholic intoxication, learning disorder, and others. These disorders are closely  
496 related to alterations of the cerebellar FC. Examples include: the dynamic FC of the  
497 cerebello-cortical affective-limbic network is associated with the severity of MDD  
498 patients<sup>33</sup>; ASD patients display decreased FC between the cerebellum and some  
499 cortical regions involved in cognitive systems<sup>63</sup>; the cerebellum is one of the brain  
500 regions most sensitive to the harmful effects of chronic alcohol abuse<sup>64</sup>, and the  
501 cerebello-cortical FC of patients with alcohol use disorder has been shown to have  
502 changes in both flexibility and integration<sup>65</sup>. Therefore, the GCI provides a possible  
503 micro-macro interacted mechanistic explanation for the engagement of the cerebellum  
504 in various neurological and neuropsychiatric disorders; i.e., one of the ways these risk  
505 genes play a role in the pathogenesis of corresponding diseases may be through their  
506 interactions with the cerebellar FC, which results in pathological manifestations as  
507 abnormalities in cerebellar functional connectivity, such as the fluctuation in the  
508 correspondence of the Gene-FC relationship found in the present study. The GCI also  
509 provides a promising genetic resource for investigating the cerebellar engagement in a  
510 range of brain diseases. For example, finding that overlapping genes, i.e., NRXN1,  
511 are associated with mental depression and autistic disorder supported previous clinical

512 studies showing that rare and common variants in NRXN1 carried risks for MDD<sup>66</sup>,  
513 ASD, and schizophrenia<sup>67</sup>, and HTR1A, which has a high expression in the  
514 cerebellum<sup>15</sup>, was found to be involved in pain, mental depression, autistic disorder,  
515 alcoholic intoxication, learning disorder, and other conditions.

### 516 *Limitations*

517 The interpretation of our findings has several caveats. First, the AHBA dataset itself  
518 has many shortcomings, although it provides an unprecedented opportunity to  
519 combine brain imaging data with genetic information. The AHBA gene expression  
520 data was obtained using microarray technology, which did not include the expression  
521 of non-encoding RNA (such as snRNA and microRNA) and lacks cellular level  
522 information because it averaged a variety of cell types within a single sample. The  
523 overall pattern of gene expression, gene regulation, epigenomics, and improved  
524 cellular resolution is helpful for fully understanding the causal relationship between  
525 genes and functional organization, which is a greater challenge for neuroscience than  
526 just identifying a link between genetic and imaging data. Second, the gene  
527 co-expression we constructed only considered one small part of the relationship  
528 between the genes and FC thereby it did not fully recapitulate the complexity of the  
529 brain transcriptome, such as gene-gene interactions<sup>68</sup>. That is one possible reason why  
530 we only found a cerebello-cortical Gene-FC correlation for the cognitive-limbic  
531 networks. Last, simple correlation approaches, such as used in this study, are only  
532 able to prioritize genes for further investigation and cannot fully explore the

533 relationship between genes and functional organization. As a result, further  
534 exploration is hindered by the intricacies of genetic and epigenetic regulation. This  
535 makes the discussion and explanation of the different directions of this correlation  
536 challenging. For example, why the direction of influence on the Gene-FC correlation  
537 could separate these 443 genes into two distinct gene sets with definitely different  
538 functions remains unclear, so further related exploration is necessary but very  
539 challenging. Nevertheless, in light of the current limited understanding of the details  
540 about how genes contribute to large-scale functional organization, the prioritization of  
541 genes and the related functional annotation presented here are still necessary and  
542 important<sup>25</sup>.

## 543 **Conclusions**

544 Overall, we found that the network-specific genes underlying cerebellar functional  
545 heterogeneity correlated with the intra-cerebellar and cerebello-cerebral FC, a finding  
546 which indicates that the genetic infrastructure associated with functional segregation  
547 coalesces to form a collective system, which has a close relationship with the  
548 functional integration of these functional subregions. The current study has thus  
549 unveiled part of the neurobiological genetic substrate underlying the cerebellar  
550 functional organization. We also identified important indirect genetic markers that  
551 support the key role played by the cerebellar functional network in many brain  
552 disorders. This hints at the possibility of establishing a “cerebellar functional  
553 abnormality – gene – disorder” loop as well as of bridging the knowledge gap

554 between the genetic mechanisms driving the cerebellar functional organization and  
555 the heritable risks of disorders, especially major depression and autistic disorder. The  
556 current study also prioritizes genes for future studies that will focus on the genetic  
557 correlates of the cerebellar functional organization, the genetic implications of  
558 cerebellar malfunction in the pathogenesis of many neurological and mental disorders,  
559 and future genetic treatment targets for the cerebellar functional abnormalities of these  
560 disorders.

## 561 **Materials and Methods**

### 562 *AHBA preprocessing*

563 The AHBA<sup>7</sup> is a publicly available transcriptome dataset (<http://www.brain-map.org>),  
564 which provides normalized microarray gene expression data from six adult donors  
565 (ages 24, 31, 34, 49, 55, and 57 years;  $n = 4$  left hemisphere only,  $n = 2$  both left and  
566 right hemispheres). Supplementary table 1 shows the demographic information.

567 The preprocessing pipeline was referred to in Anderson et al.<sup>27</sup>, and included data  
568 filtering, probe selection, sample selection, and assignment. We first filtered the  
569 probes with the AHBA binary indicator to mitigate the background noise and  
570 excluded probes without an Entrez ID. Then for the genes that corresponded to two or  
571 more probes, we chose the probe with the maximum summed adjacency to represent  
572 the corresponding gene expression; otherwise the probe with the highest mean  
573 expression was retained, using the CollapseRows function<sup>69</sup> in R. The first two steps

574 generated 20,738 unique mRNA probes, which provided expression data for 20,738  
575 genes. As suggested by Arnatkeviciute et al.<sup>70</sup> and given the known transcriptional  
576 differences<sup>14</sup> between the cortical and sub-cortical regions and the cerebellum, we  
577 separated the cortical and cerebellar samples a priori based on the slab type and  
578 structure name provided by AHBA and processed them separately later. In the end,  
579 337 samples were retained for the cerebellar cortex and 1,701 samples for the cortical  
580 cortex.

581 Finally, we respectively assigned these 337 cerebellum samples and 1,701  
582 cortical samples into the cerebellar functional network atlas<sup>22</sup> and cortical functional  
583 networks atlas<sup>29</sup>, both of which have 7- and 17-network parcellation strategies. For  
584 each cerebellar sample, we first generated a single  $1 \times 1 \times 1 \text{ mm}^3$  region of interest  
585 (ROI) at the MNI coordinate for each sample using AFNI<sup>71</sup>. The network label from  
586 either region 7 or 17 was assigned, if the ROI fell within a cerebellar network of the  
587 Buckner atlas. Considering the uneven and discrete sampling of the AHBA data<sup>7</sup>, if  
588 the  $1 \times 1 \times 1 \text{ mm}^3$  ROI did not overlap with any network, the associated ROI was  
589 expanded to  $3 \times 3 \times 3 \text{ mm}^3$ , and if the  $3 \times 3 \times 3 \text{ mm}^3$  ROI overlapped with the  
590 functional atlas, the network that had the maximum number of shared voxels with the  
591 ROI was assigned. Otherwise, the steps above were repeated for a  $5 \times 5 \times 5 \text{ mm}^3$  ROI.  
592 The cerebellar samples were excluded ( $n = 22$ ) if the  $5 \times 5 \times 5 \text{ mm}^3$  ROI did not  
593 overlap with any cerebellar networks. Supplementary tables 2 and 3 show the  
594 distributions of the cerebellar sample assignment for the 7-network and 17-network  
595 atlases. The assignment of the AHBA cortical samples into the cortical functional



596 network atlas was consistent with the method used for the cerebellum, and the cortical  
597 sample distributions are shown in Supplementary tables 4 and 5.

### 598 *Differential gene expression analysis across functional networks*

599 The gene expressions of the cerebellar samples within the same network were  
600 averaged for each gene across the samples, resulting in 20738 genes  $\times$  7 or 17  
601 network matrices for each donor. Then we calculated the differential gene expression  
602 across the 7 networks using the R limma package<sup>28</sup> by comparing the gene expression  
603 in one network (e.g., control) with the remaining 6 networks (e.g., default, limbic,  
604 visual, etc.). The traditional minimum fold change threshold was not suitable for  
605 determining biologically meaningful but subtly different expressions<sup>42</sup>. Instead, we  
606 applied the Benjamini-Hochberg (BH) method to control the false discovery rate  
607 (FDR), and the FDR corrected statistical threshold  $q \leq .05$  combined with a fold  
608 change  $> 0$  was used as the key indicator for differentially expressed genes. The  
609 residual donor effects were accounted for by using limma's duplicateCorrelation  
610 tool<sup>28</sup>. For simplicity, the genes that were differentially expressed across cerebellar  
611 networks are referred to as cerebellar network-specific genes throughout this paper.  
612 The cortical network-specific genes were identified in the same way. The only  
613 difference was that the gene expression of the cortical samples was first averaged  
614 within each parcel (51 and 114 parcels, which corresponded to the 7- and 17-networks,  
615 respectively)<sup>29</sup> and then averaged within each network.

616 *Cerebellar resting-state functional connectivity (rsFC)*

617 The minimally preprocessed<sup>72,73</sup> Human Connectome Project (HCP) S1200 release  
618 dataset<sup>31</sup>, which has 1,018 subjects with both structural MRI and resting-state  
619 functional MRI (rs-fMRI, HCP S1200 manual), was used. The preprocessing pipeline  
620 includes artifact correction (correction of gradient nonlinearity distortion, realignment  
621 for head motion, registration of fMRI data using structural data, reduction of  
622 geometric distortions due to B0 field inhomogeneity, etc.) as well as denoising by  
623 ICA-FIX<sup>74,75</sup>. Time courses were extracted from these CIFTI grayordinate-format  
624 preprocessed rs-fMRI images, and the global signal was regressed as well. The  
625 resting-state BOLD time series were averaged within each cortical parcel of the 7- or  
626 17-network cortical atlases and within each cerebellar network of the 7- or  
627 17-network cerebellar atlases<sup>22</sup>, separately. The rsFC within the cerebellum was  
628 computed using the Pearson's correlation for the averaged time courses for each ROI  
629 of interest. Because four runs were performed for each subject, the correlation values  
630 were separately calculated for each run, Fisher's z-transformed, and averaged across  
631 the runs, resulting in a 17 × 17 networks matrix. The same process was used to  
632 calculate the correlations between each functional cerebellar network and each  
633 cortical parcel, resulting in a 114 cortical parcels × 7 cerebellar networks functional  
634 correlation matrix, which represents the rsFC across the cerebello-cortical circuit.  
635 Regardless of whether the FC was within the cerebellum or across the  
636 cerebello-cortical circuit, both categories of FC were defined using the more

637 fine-grained 17-network parcellation to increase the spatial resolution. The only  
638 exception was that the cerebellar 7-network was applied while calculating the FC  
639 across the cerebello-cortical circuit to compare each cerebellar network more directly.

#### 640 *Correlation between gene co-expression with intra-cerebellar rsFC*

641 To fully capture the genetic correlation with the FC within the cerebellum, we  
642 leveraged the genetic samples of the 2 bi-hemisphere donors when constructing the  
643 gene co-expression matrix because the rsFC of the cerebellum is bilateral. Therefore,  
644 the gene co-expression was analyzed for the 2 bi-hemisphere donors using the 443  
645 differentially expressed genes derived from all 6 donors across 7 networks, using a  
646 finer 17-network parcellation to increase the spatial resolution. Ten networks that  
647 contained samples from both bi-hemisphere donors were retained (Table S3). For each  
648 bi-hemispheric donor, the log<sub>2</sub> gene expression of the cerebellar samples was  
649 mean-normalized and then averaged within each network. The cerebellar 10 × 10  
650 networks correlation matrix was calculated using the Spearman's correlations  
651 individually, then Fisher transformed, and finally averaged to construct the final 10  
652 networks gene co-expression matrix. The correlation significance level of the gene  
653 co-expression was evaluated using the overlap between the correlation matrix for  
654 these two individuals and adjusted by Bonferroni correction. Meanwhile, we  
655 transformed the 17 × 17 networks rsFC matrix into a 10 × 10 networks size to be  
656 consistent with the gene co-expression matrix. Finally, the relationship between the 10  
657 × 10 networks gene co-expression and the 10 × 10 networks rsFC matrix was

658 computed using Pearson's correlation. The correlation between the gene  
659 co-expression and FC is referred to as the Gene-FC correlation throughout the present  
660 paper for simplicity.

661 To test whether these Gene-FC relationships were identified by chance, we  
662 randomly shuffled the network labels of each cerebellar sample 10,000 times, kept the  
663 distribution probability of the sample in each network consistent, and then  
664 reperformed the previous analyses with the same criteria for each permutation. In  
665 addition, to confirm that the verified Gene-FC correlation within the cerebellum is  
666 meaningful and to evaluate its robustness, we also recalculated it using several  
667 different parcellations, i.e., a task-free 7-network parcellation, independent task-based  
668 multi-domain task battery (MDTB) functional parcellation<sup>21</sup>, and cerebellar lobular  
669 parcellation<sup>30</sup>. The criteria for each step were consistent with our main method. Lastly,  
670 we employed a control test to learn whether the Gene-FC correlation could be  
671 obtained using only the network-specific genes, that is, no Gene-FC correlation while  
672 using other genes. We randomly select 443 genes from the full gene set without the  
673 network-specific genes and referred to them as non-network-specific genes. Then we  
674 calculated the Gene-FC correlation using the non-network-specific genes and ran this  
675 step randomly 10,000 times. In addition to these thresholdless non-network-specific  
676 genes, we applied a set of thresholds to the averaged original log<sub>2</sub> gene expression  
677 data to confirm that these non-network-specific genes were expressed in the  
678 cerebellum and to test whether the gene co-expression pattern constructed using these  
679 threshold non-network-specific genes was correlated with FC.

680 *Correlation between gene co-expression and rsFC across the cerebello-cortical*  
681 *circuit*

682 To fully investigate the cerebellar functional organization, we also explored the  
683 relationship between the cerebello-cortical FC and the genetic correlation based on  
684 the strategy used in Anderson et al.<sup>27</sup>. First, we defined the network-specific genes in  
685 the cortex using the same procedure as we had for the cerebellum and examined the  
686 genes that overlapped within the same network of the cerebellum and the cortex using  
687 a hypergeometric test. Then the gene co-expression matrix was constructed between 6  
688 cerebellar networks and 59 cortical parcels from the 2 bi-hemisphere donors, using  
689 the 90 unique genes derived from the overlap between the cortical network-specific  
690 genes and the cerebellar network-specific genes. Here, the cerebellar 7-network  
691 parcellation was selected to compare the different cerebellar networks more directly.  
692 The visual network was excluded because it only had two samples that were solely  
693 from one of the 2 bi-hemisphere donors. For the cerebral cortex, 59 cortical parcels  
694 that contained samples from both bi-hemisphere donors were estimated. The log<sub>2</sub>  
695 mean-normalized expression within each cerebellar network and each cortical parcel  
696 was estimated individually and correlated using Spearman's  $\rho$ , Fisher-transformed,  
697 and averaged. We transformed the 114 cortical parcels  $\times$  7 cerebellar networks rsFC  
698 matrix into 59 cortical parcels  $\times$  6 cerebellar networks size to be consistent with the  
699 gene co-expression matrix. Finally, the relationship between the cortical genetic  
700 correlation and the cerebello-cortical rsFC matrix was computed using Pearson's

701 correlation across 6 cerebellar networks and adjusted by the Benjamini-Hochberg  
702 method to correct for multiple comparisons.

### 703 ***Gene functional annotation***

#### 704 *Virtual Gene Knock-out (KO)*

705 To extend our investigation of the overall relationship between gene co-expression  
706 and FC within the cerebellum, we referred to a similar previous approach<sup>76,77</sup> and  
707 termed it the “Virtual Gene Knock-out (KO)” to evaluate each gene’s contribution to  
708 the Gene-FC correlation. In brief, we deleted each of the 443 cerebellar  
709 network-specific genes one-by-one to simulate the gene knock-out, then constructed  
710 the gene co-expression matrix without that gene, analyzed the correlation between the  
711 FC and the gene co-expression, and finally calculated the difference in the correlation  
712 coefficient between before and after the simulated deletion, with the result being  
713 defined as the gene contribution indicator (GCI). Based on the GCI, we identified two  
714 different gene sets that had opposite effects on the Gene-FC correlation: a GCI  
715 positive gene set (GCI<sup>+</sup>) and a GCI negative gene set (GCI<sup>-</sup>). The virtual KO of GCI<sup>+</sup>  
716 increased the Gene-FC correlation, and, accordingly, its expression decreased the  
717 Gene-FC correlation; in contrast, the virtual KO of GCI<sup>-</sup> decreased the correlation,  
718 and, accordingly, its expression increased the Gene-FC correlation.

#### 719 *GO, pathway, and disorder enrichment analysis (ToppGene portal)*

720 To characterize the biological role of GCI<sup>+</sup> and GCI<sup>-</sup>, we applied the ToppGene

721 portal<sup>78</sup> to conduct a gene ontology (GO), pathway, and disorder enrichment analysis.  
722 The Benjamini-Hochberg method for false discovery rate (FDR-BH correction) ( $q$   
723  $< .05$ ) was chosen to correct for multiple comparisons.

#### 724 *Spatial-Temporal Analysis*

725 To investigate the overall spatial-temporal expression features of these genes, we  
726 applied an online cell type-specific expression analysis (CSEA) tool<sup>36</sup> to do the  
727 enrichment analysis of the genes within the cerebellum during different lifespan  
728 windows. Here, a specificity index probability ( $pSI = .05, .01, .001, \text{ and } .0001$ ,  
729 permutation corrected) was used to define the probability of a gene being expressed in  
730 each time window relative to all other time windows to represent the varying  
731 stringencies for enrichment. The significance of the overlap between the interest gene  
732 set and those enriched in a specific time window was evaluated by Fisher's exact test,  
733 and the Benjamini-Hochberg method for false discovery rate (FDR-BH correction)  
734 was chosen to correct for multiple comparisons.

#### 735 **Acknowledgments**

736 This work was partially supported by the Natural Science Foundation of China (Grant  
737 Nos. 82072099, 91432302, and 31620103905), the Strategic Priority Research  
738 Program of Chinese Academy of Sciences (XDB32030200), National Key R&D  
739 Program of China (Grant No. 2017YFA0105203), Beijing Municipal Science &  
740 Technology Commission (Grant Nos. Z161100000216152, Z171100000117002), the  
741 Youth Innovation Promotion Association, and the Beijing Advanced Discipline Fund.

742 The authors appreciate the English language and editing assistance of Rhoda E. and  
743 Edmund F. Perozzi, PhDs.

## 744 **Conflict of Interest**

745 The authors declare that the research was conducted in the absence of any commercial  
746 or financial relationships that could be construed as a potential conflict of interest.

## 747 **Supplementary Material**

748 Shown in supplementary figures and supplementary sheets.

## 749 **Data availability**

750 R 3.6.1 and custom scripts were used to perform statistical analysis, all R packages  
751 were mentioned explicitly in the text where the package was used. The analysis code  
752 is freely available (<https://github.com/FANLabCASIA/CerebellarGeneFCCorrelation>).  
753 The ToppGene website (<https://toppgene.cchmc.org/>) and CSEA tool  
754 (<http://genetics.wustl.edu/jdlab/csea-tool-2/>) which used to do the functional  
755 annotation of genes were all freely accessible. A Supplementary Data file provides  
756 complete gene lists, the output of differential expression, rs-fMRI, genetic correlation,  
757 validation results, and functional annotation results.



## 758 References

- 759 1 Schmahmann, J. D., Guell, X., Stoodley, C. J. & Halko, M. A. The Theory and  
760 Neuroscience of Cerebellar Cognition. *Annu Rev Neurosci* **42**, 337-364,  
761 doi:10.1146/annurev-neuro-070918-050258 (2019).
- 762 2 De Zeeuw, C. I., Lisberger, S. G. & Raymond, J. L. Diversity and dynamism  
763 in the cerebellum. *Nat Neurosci* **24**, 160-167,  
764 doi:10.1038/s41593-020-00754-9 (2021).
- 765 3 Sathyanesan, A. *et al.* Emerging connections between cerebellar development,  
766 behaviour and complex brain disorders. *Nat Rev Neurosci* **20**, 298-313,  
767 doi:10.1038/s41583-019-0152-2 (2019).
- 768 4 Guell, X., Schmahmann, J. D. & Gabrieli, J. D. E. Functional Specialization is  
769 Independent of Microstructural Variation in Cerebellum but Not in Cerebral  
770 Cortex. *bioRxiv*, 424176, doi:10.1101/424176 (2018).
- 771 5 Voogd, J. & Glickstein, M. The anatomy of the cerebellum. *Trends in*  
772 *Cognitive Sciences* **2**, 307-313,  
773 doi:[https://doi.org/10.1016/S1364-6613\(98\)01210-8](https://doi.org/10.1016/S1364-6613(98)01210-8) (1998).
- 774 6 Schmahmann, J. D. The role of the cerebellum in affect and psychosis.  
775 *Journal of Neurolinguistics* **13**, 189-214,  
776 doi:[https://doi.org/10.1016/S0911-6044\(00\)00011-7](https://doi.org/10.1016/S0911-6044(00)00011-7) (2000).
- 777 7 Hawrylycz, M. J. *et al.* An anatomically comprehensive atlas of the adult  
778 human brain transcriptome. *Nature* **489**, 391-399, doi:10.1038/nature11405  
779 (2012).
- 780 8 Johnson, M. B. *et al.* Functional and evolutionary insights into human brain  
781 development through global transcriptome analysis. *Neuron* **62**, 494-509,  
782 doi:10.1016/j.neuron.2009.03.027 (2009).
- 783 9 Guevara, E. E. *et al.* Comparative analysis reveals distinctive epigenetic  
784 features of the human cerebellum. *PLoS Genet* **17**, e1009506,  
785 doi:10.1371/journal.pgen.1009506 (2021).
- 786 10 Wang, V. Y. & Zoghbi, H. Y. Genetic regulation of cerebellar development.  
787 *Nat Rev Neurosci* **2**, 484-491, doi:10.1038/35081558 (2001).
- 788 11 Schmahmann, J. D. The cerebellum and cognition. *Neurosci Lett* **688**, 62-75,  
789 doi:10.1016/j.neulet.2018.07.005 (2019).
- 790 12 Phillips, J. R., Hewedi, D. H., Eissa, A. M. & Moustafa, A. A. The cerebellum  
791 and psychiatric disorders. *Front Public Health* **3**, 66,  
792 doi:10.3389/fpubh.2015.00066 (2015).
- 793 13 Diwakar, S. Cerebellum in Neurological Disorders: A Review on the Role of  
794 Inter-Connected Neural Circuits. *Journal of Neurology & Stroke* **6**,  
795 doi:10.15406/jnsk.2017.06.00196 (2017).
- 796 14 Hawrylycz, M. *et al.* Canonical genetic signatures of the adult human brain.  
797 *Nat Neurosci* **18**, 1832-1844, doi:10.1038/nn.4171 (2015).
- 798 15 Negi, S. K. & Guda, C. Global gene expression profiling of healthy human

- 799 brain and its application in studying neurological disorders. *Sci Rep* **7**, 897,  
800 doi:10.1038/s41598-017-00952-9 (2017).
- 801 16 Aldinger, K. A. *et al.* Spatial and cell type transcriptional landscape of human  
802 cerebellar development. *Nat Neurosci*, doi:10.1038/s41593-021-00872-y  
803 (2021).
- 804 17 Zeng, T. *et al.* Allen mouse brain atlases reveal different neural connection and  
805 gene expression patterns in cerebellum gyri and sulci. *Brain Struct Funct* **220**,  
806 2691-2703, doi:10.1007/s00429-014-0821-x (2015).
- 807 18 Kozareva, V. *et al.* A transcriptomic atlas of the mouse cerebellum reveals  
808 regional specializations and novel cell types. *bioRxiv*, 2020.2003.2004.976407,  
809 doi:10.1101/2020.03.04.976407 (2020).
- 810 19 Ren, Y., Guo, L. & Guo, C. C. A connectivity-based parcellation improved  
811 functional representation of the human cerebellum. *Sci Rep* **9**, 9115,  
812 doi:10.1038/s41598-019-45670-6 (2019).
- 813 20 Bernard, J. A. *et al.* Resting state cortico-cerebellar functional connectivity  
814 networks: a comparison of anatomical and self-organizing map approaches.  
815 *Front Neuroanat* **6**, 31, doi:10.3389/fnana.2012.00031 (2012).
- 816 21 King, M., Hernandez-Castillo, C. R., Poldrack, R. A., Ivry, R. B. &  
817 Diedrichsen, J. Functional boundaries in the human cerebellum revealed by a  
818 multi-domain task battery. *Nat Neurosci* **22**, 1371-1378,  
819 doi:10.1038/s41593-019-0436-x (2019).
- 820 22 Buckner, R. L., Krienen, F. M., Castellanos, A., Diaz, J. C. & Yeo, B. T. The  
821 organization of the human cerebellum estimated by intrinsic functional  
822 connectivity. *J Neurophysiol* **106**, 2322-2345, doi:10.1152/jn.00339.2011  
823 (2011).
- 824 23 Ji, J. L. *et al.* Mapping the human brain's cortical-subcortical functional  
825 network organization. *Neuroimage* **185**, 35-57,  
826 doi:10.1016/j.neuroimage.2018.10.006 (2019).
- 827 24 Guell, X., Schmahmann, J. D., Gabrieli, J. & Ghosh, S. S. Functional  
828 gradients of the cerebellum. *Elife* **7**, doi:10.7554/eLife.36652 (2018).
- 829 25 Fornito, A., Arnatkeviciute, A. & Fulcher, B. D. Bridging the Gap between  
830 Connectome and Transcriptome. *Trends Cogn Sci* **23**, 34-50,  
831 doi:10.1016/j.tics.2018.10.005 (2019).
- 832 26 Richiardi, J. *et al.* BRAIN NETWORKS. Correlated gene expression supports  
833 synchronous activity in brain networks. *Science* **348**, 1241-1244,  
834 doi:10.1126/science.1255905 (2015).
- 835 27 Anderson, K. M. *et al.* Gene expression links functional networks across  
836 cortex and striatum. *Nat Commun* **9**, 1428, doi:10.1038/s41467-018-03811-x  
837 (2018).
- 838 28 Ritchie, M. E. *et al.* limma powers differential expression analyses for  
839 RNA-sequencing and microarray studies. *Nucleic Acids Res* **43**, e47,  
840 doi:10.1093/nar/gkv007 (2015).
- 841 29 Yeo, B. T. *et al.* The organization of the human cerebral cortex estimated by

- 842 intrinsic functional connectivity. *J Neurophysiol* **106**, 1125-1165,  
843 doi:10.1152/jn.00338.2011 (2011).
- 844 30 Diedrichsen, J., Balsters, J. H., Flavell, J., Cussans, E. & Ramnani, N. A  
845 probabilistic MR atlas of the human cerebellum. *Neuroimage* **46**, 39-46,  
846 doi:10.1016/j.neuroimage.2009.01.045 (2009).
- 847 31 Van Essen, D. C. *et al.* The Human Connectome Project: a data acquisition  
848 perspective. *Neuroimage* **62**, 2222-2231,  
849 doi:10.1016/j.neuroimage.2012.02.018 (2012).
- 850 32 Huntley, R. P. *et al.* The GOA database: gene Ontology annotation updates for  
851 2015. *Nucleic Acids Res* **43**, D1057-1063, doi:10.1093/nar/gku1113 (2015).
- 852 33 Zhu, D. M. *et al.* Cerebellar-cerebral dynamic functional connectivity  
853 alterations in major depressive disorder. *J Affect Disord* **275**, 319-328,  
854 doi:10.1016/j.jad.2020.06.062 (2020).
- 855 34 Verly, M. *et al.* Altered functional connectivity of the language network in  
856 ASD: role of classical language areas and cerebellum. *Neuroimage Clin* **4**,  
857 374-382, doi:10.1016/j.nicl.2014.01.008 (2014).
- 858 35 Miller, J. A. *et al.* Transcriptional landscape of the prenatal human brain.  
859 *Nature* **508**, 199-206, doi:10.1038/nature13185 (2014).
- 860 36 Dougherty, J. D., Schmidt, E. F., Nakajima, M. & Heintz, N. Analytical  
861 approaches to RNA profiling data for the identification of genes enriched in  
862 specific cells. *Nucleic Acids Res* **38**, 4218-4230, doi:10.1093/nar/gkq130  
863 (2010).
- 864 37 ten Donkelaar, H. J., Lammens, M., Wesseling, P., Thijssen, H. O. & Renier, W.  
865 O. Development and developmental disorders of the human cerebellum. *J*  
866 *Neurol* **250**, 1025-1036, doi:10.1007/s00415-003-0199-9 (2003).
- 867 38 Munoz-Castaneda, R. *et al.* Cytoskeleton stability is essential for the integrity  
868 of the cerebellum and its motor- and affective-related behaviors. *Sci Rep* **8**,  
869 3072, doi:10.1038/s41598-018-21470-2 (2018).
- 870 39 Beyreli, I., Karakahya, O. & Cicek, A. E. Deep multitask learning of gene risk  
871 for comorbid neurodevelopmental disorders. *bioRxiv*, 2020.2006.2013.150201,  
872 doi:10.1101/2020.06.13.150201 (2020).
- 873 40 Villarroel, M. A. & Terlizzi, E. P. Symptoms of Depression Among Adults:  
874 United States, 2019. *NCHS Data Brief*, 1-8 (2020).
- 875 41 Anderson, M. L., Kinnison, J. & Pessoa, L. Describing functional diversity of  
876 brain regions and brain networks. *Neuroimage* **73**, 50-58,  
877 doi:10.1016/j.neuroimage.2013.01.071 (2013).
- 878 42 Dalman, M. R., Deeter, A., Nimishakavi, G. & Duan, Z.-H. Fold change and  
879 p-value cutoffs significantly alter microarray interpretations. *BMC*  
880 *Bioinformatics* **13**, S11, doi:10.1186/1471-2105-13-S2-S11 (2012).
- 881 43 Margulies, D. S. *et al.* Situating the default-mode network along a principal  
882 gradient of macroscale cortical organization. *Proc Natl Acad Sci U S A* **113**,  
883 12574-12579, doi:10.1073/pnas.1608282113 (2016).
- 884 44 Schmahmann, J. D. & Pandya, D. N. Disconnection syndromes of basal

- 885 ganglia, thalamus, and cerebrocerebellar systems. *Cortex* **44**, 1037-1066,  
886 doi:10.1016/j.cortex.2008.04.004 (2008).
- 887 45 Schmahmann, J. D. From movement to thought: anatomic substrates of the  
888 cerebellar contribution to cognitive processing. *Hum Brain Mapp* **4**, 174-198,  
889 doi:10.1002/(SICI)1097-0193(1996)4:3<174::AID-HBM3>3.0.CO;2-0  
890 (1996).
- 891 46 Storbeck, J. & Clore, G. L. On the interdependence of cognition and emotion.  
892 *Cogn Emot* **21**, 1212-1237, doi:10.1080/02699930701438020 (2007).
- 893 47 Ghashghaei, H. T. & Barbas, H. Pathways for emotion: interactions of  
894 prefrontal and anterior temporal pathways in the amygdala of the rhesus  
895 monkey. *Neuroscience* **115**, 1261-1279,  
896 doi:[https://doi.org/10.1016/S0306-4522\(02\)00446-3](https://doi.org/10.1016/S0306-4522(02)00446-3) (2002).
- 897 48 Riener, C. R., Stefanucci, J. K., Proffitt, D. R. & Clore, G. An effect of mood  
898 on the perception of geographical slant. *Cogn Emot* **25**, 174-182,  
899 doi:10.1080/02699931003738026 (2011).
- 900 49 Mueller, S. *et al.* Individual variability in functional connectivity architecture  
901 of the human brain. *Neuron* **77**, 586-595, doi:10.1016/j.neuron.2012.12.028  
902 (2013).
- 903 50 Guell, X., Schmahmann, J. D. & Gabrieli, J. D. Functional Specialization is  
904 Independent of Microstructural Variation in Cerebellum but Not in Cerebral  
905 Cortex. *bioRxiv*, 424176, doi:10.1101/424176 (2018).
- 906 51 Marek, S. *et al.* Spatial and Temporal Organization of the Individual Human  
907 Cerebellum. *Neuron* **100**, 977-993 e977, doi:10.1016/j.neuron.2018.10.010  
908 (2018).
- 909 52 Hensler, J. G. Serotonergic modulation of the limbic system. *Neurosci*  
910 *Biobehav Rev* **30**, 203-214, doi:10.1016/j.neubiorev.2005.06.007 (2006).
- 911 53 Schmahmann, J. D. Disorders of the Cerebellum: Ataxia, Dysmetria of  
912 Thought, and the Cerebellar Cognitive Affective Syndrome. *The Journal of*  
913 *Neuropsychiatry and Clinical Neurosciences* **16**, 367-378,  
914 doi:10.1176/jnp.16.3.367 (2004).
- 915 54 Brainstorm, C. *et al.* Analysis of shared heritability in common disorders of  
916 the brain. *Science* **360**, doi:10.1126/science.aap8757 (2018).
- 917 55 Bertoli-Avella, A. M. *et al.* Biallelic inactivating variants in the GTPBP2 gene  
918 cause a neurodevelopmental disorder with severe intellectual disability. *Eur J*  
919 *Hum Genet* **26**, 592-598, doi:10.1038/s41431-018-0097-3 (2018).
- 920 56 Wefers, A. K., Lindner, S., Schulte, J. H. & Schuller, U. Overexpression of  
921 Lin28b in Neural Stem Cells is Insufficient for Brain Tumor Formation, but  
922 Induces Pathological Lobulation of the Developing Cerebellum. *Cerebellum*  
923 **16**, 122-131, doi:10.1007/s12311-016-0774-0 (2017).
- 924 57 Swoboda, K. J. & Hyland, K. Diagnosis and treatment of  
925 neurotransmitter-related disorders. *Neurol Clin* **20**, 1143-1161, viii,  
926 doi:10.1016/s0733-8619(02)00018-x (2002).
- 927 58 Brown, R. P. & Mann, J. J. A clinical perspective on the role of

- 928 neurotransmitters in mental disorders. *Hosp Community Psychiatry* **36**,  
929 141-150, doi:10.1176/ps.36.2.141 (1985).
- 930 59 Kato, T. A. *et al.* Neurotransmitters, psychotropic drugs and microglia: clinical  
931 implications for psychiatry. *Curr Med Chem* **20**, 331-344,  
932 doi:10.2174/0929867311320030003 (2013).
- 933 60 Seo, D., Patrick, C. J. & Kennealy, P. J. Role of Serotonin and Dopamine  
934 System Interactions in the Neurobiology of Impulsive Aggression and its  
935 Comorbidity with other Clinical Disorders. *Aggress Violent Behav* **13**, 383-395,  
936 doi:10.1016/j.avb.2008.06.003 (2008).
- 937 61 Su, Y., D'Arcy, C. & Meng, X. Research Review: Developmental origins of  
938 depression - a systematic review and meta-analysis. *J Child Psychol*  
939 *Psychiatry*, doi:10.1111/jcpp.13358 (2020).
- 940 62 Newschaffer, C. J., Fallin, D. & Lee, N. L. Heritable and nonheritable risk  
941 factors for autism spectrum disorders. *Epidemiol Rev* **24**, 137-153,  
942 doi:10.1093/epirev/mxf010 (2002).
- 943 63 Ramos, T. C., Balardin, J. B., Sato, J. R. & Fujita, A. Abnormal  
944 Cortico-Cerebellar Functional Connectivity in Autism Spectrum Disorder.  
945 *Front Syst Neurosci* **12**, 74, doi:10.3389/fnsys.2018.00074 (2018).
- 946 64 Baker, K. G., Harding, A. J., Halliday, G. M., Kril, J. J. & Harper, C. G.  
947 Neuronal loss in functional zones of the cerebellum of chronic alcoholics with  
948 and without Wernicke's encephalopathy. *Neuroscience* **91**, 429-438,  
949 doi:10.1016/s0306-4522(98)90664-9 (1999).
- 950 65 Abdallah, M. *et al.* Altered Cerebro-Cerebellar Dynamic Functional  
951 Connectivity in Alcohol Use Disorder: a Resting-State fMRI Study.  
952 *Cerebellum*, doi:10.1007/s12311-021-01241-y (2021).
- 953 66 Freire-Cobo, C. & Wang, J. Dietary phytochemicals modulate  
954 experience-dependent changes in Neurexin gene expression and alternative  
955 splicing in mice after chronic variable stress exposure. *Eur J Pharmacol* **883**,  
956 173362, doi:10.1016/j.ejphar.2020.173362 (2020).
- 957 67 Hu, Z., Xiao, X., Zhang, Z. & Li, M. Genetic insights and neurobiological  
958 implications from NRXN1 in neuropsychiatric disorders. *Molecular*  
959 *Psychiatry* **24**, 1400-1414, doi:10.1038/s41380-019-0438-9 (2019).
- 960 68 Hua, J., Yang, Z., Jiang, T. & Yu, S. Pair-wise interactions in gene expression  
961 determine a hierarchical transcription profile of human brain. *Science Bulletin*,  
962 doi:<https://doi.org/10.1016/j.scib.2021.01.003> (2021).
- 963 69 Miller, J. A. *et al.* Strategies for aggregating gene expression data: the  
964 collapseRows R function. *BMC Bioinformatics* **12**, 322,  
965 doi:10.1186/1471-2105-12-322 (2011).
- 966 70 Arnatkeviciute, A., Fulcher, B. D. & Fornito, A. A practical guide to linking  
967 brain-wide gene expression and neuroimaging data. *Neuroimage* **189**, 353-367,  
968 doi:10.1016/j.neuroimage.2019.01.011 (2019).
- 969 71 Cox, R. W. AFNI: software for analysis and visualization of functional  
970 magnetic resonance neuroimages. *Computers and biomedical research, an*

- 971 *international journal* **29**, 162-173, doi:10.1006/cbmr.1996.0014 (1996).
- 972 72 Smith, S. M. *et al.* Resting-state fMRI in the Human Connectome Project.  
973 *Neuroimage* **80**, 144-168, doi:10.1016/j.neuroimage.2013.05.039 (2013).
- 974 73 Glasser, M. F. *et al.* The minimal preprocessing pipelines for the Human  
975 Connectome Project. *Neuroimage* **80**, 105-124,  
976 doi:10.1016/j.neuroimage.2013.04.127 (2013).
- 977 74 Salimi-Khorshidi, G. *et al.* Automatic denoising of functional MRI data:  
978 combining independent component analysis and hierarchical fusion of  
979 classifiers. *Neuroimage* **90**, 449-468, doi:10.1016/j.neuroimage.2013.11.046  
980 (2014).
- 981 75 Griffanti, L. *et al.* ICA-based artefact removal and accelerated fMRI  
982 acquisition for improved resting state network imaging. *Neuroimage* **95**,  
983 232-247, doi:10.1016/j.neuroimage.2014.03.034 (2014).
- 984 76 Kong, X.-Z. *et al.* Gene Expression Correlates of the Cortical Network  
985 Underlying Sentence Processing. *Neurobiology of Language* **1**, 77-103,  
986 doi:10.1162/nol\_a\_00004 (2020).
- 987 77 Seidlitz, J. *et al.* Morphometric Similarity Networks Detect Microscale  
988 Cortical Organization and Predict Inter-Individual Cognitive Variation. *Neuron*  
989 **97**, 231-247 e237, doi:10.1016/j.neuron.2017.11.039 (2018).
- 990 78 Chen, J., Bardes, E. E., Aronow, B. J. & Jegga, A. G. ToppGene Suite for gene  
991 list enrichment analysis and candidate gene prioritization. *Nucleic Acids Res*  
992 **37**, W305-311, doi:10.1093/nar/gkp427 (2009).
- 993